https://doi.org/10.1590/jatm.v18.1442

ORIGINAL PAPER

# Low Speed Aerodynamic Performance Experimental Study of NACA 23012 Half-Span Wing

Afaq Altaf[1], Mohammed Abdulmalek Mohammed Aldheeb[2,*], Ashraf Ali Omar[3], Waqar Asrar[4]

1. Emirates Aviation University – Faculty of Engineering – Dubai – United Arab Emirates.
2. International Islamic University Malaysia – Kulliyyah of Engineering – Department of Mechanical and Aerospace Engineering – Kuala Lumpur – Malaysia.
3. International University of Rabat – School of Aerospace and Automotive Engineering – Rabat – Morocco.
4. Eastern Michigan University – GameAbove College of Engineering & Technology – Ypsilanti/MI – USA.

*Corresponding author: aldheeb@iium.edu.my

## ABSTRACT

A six-component force balance was used to obtain the aerodynamic performance of a NACA 23012 half-span wing model at low freestream speeds of 20 m·s$^{-1}$ to 50 m·s$^{-1}$. The half-span wing model is equipped with a leading-edge slat and a trailing-edge flap. The impact on aerodynamic performance by the slat and flap configurations of the half-span wing model is studied. Abundant high Reynolds number aerodynamic performance studies have been carried out on various well-known airfoil profiles, but low-speed aerodynamic performance studies are limited. This work will be used as a benchmark study to support researchers working on NACA 23012 airfoils or wings at low speeds.

**Keywords:** NACA 23012; Aerodynamic performance; Slat; Flap; High lift configuration.

## INTRODUCTION

The aerodynamic performance of airfoils is essential to the design of aircraft wings. NACA 23012 is a well-known airfoil used in low-speed aircraft design due to its desirable aerodynamic characteristics.

NACA 23012 is a cambered airfoil known for its excellent lift and drag properties, particularly at low Reynolds numbers. It features a maximum thickness of 12% and a maximum camber of 2%, located at 30% chord.

The NACA 23012 airfoil is popular in the aviation industry for its high lift-to-drag ratio, making it a common choice. Its aerodynamic performance is attributed to a thick leading edge and a curved upper surface, creating a low-pressure zone on top and a high-pressure area underneath. This pressure difference generates the lift necessary for flight. The airfoil's design, featuring significant camber and thickness near the leading edge, enhances its performance at low speeds, making it ideal for slow-speed operations and maneuverability.

Several studies have investigated the aerodynamic performance of the NACA 23012 airfoil and wing, using diverse research methods such as experimental and numerical analyses. One comprehensive study conducted by Addy Jr. *et al.* (2016) involved collaboration between the National Aeronautics and Space Administration, Office National d'Études et de Recherches Aérospatiales, and the University of Illinois. They established benchmark databases of ice accretions and their impact on aerodynamics. To achieve this, large wind tunnel campaigns utilized both full-scale and subscale models of the airfoil, aiding in the study of aircraft icing effects and the development of ice-accretion prediction codes.

**Received:** Feb. 27, 2025 | **Accepted:** Apr. 17, 2026
**Peer Review History:** Single Blind Peer Review.
**Section editor:** SungKi Jung

Yoo (2000) conducted a numerical investigation exploring the influence of the Gurney flap on the NACA 23012 airfoil. The findings demonstrated that the Gurney flap led to improved lift and drag values, resulting in an enhanced lift-to-drag ratio, especially at low angles of attack and high lift coefficients. Similarly, Cavanaugh *et al.* (2007) performed wind tunnel experiments on a NACA 23012 wing equipped with Gurney flaps and trailing-edge T-strips. The experiment revealed that the flaps increased lift, and the drag increment exhibited a non-linear relationship dependent on their height. Gabbasa *et al.* (2013) used the computational fluid dynamics (CFD) method to obtain the aerodynamic performance of a multi-element NACA 23012 airfoil. The outcome of aerodynamic performance showed agreement with experimental data. Jun *et al.* (2014) investigated the flow over a three-dimensional ice-shaped model on NACA 23012 using CFD. The outcome shows a correlation between CFD and experimental data for rime ice accretion simulations.

Todorov (2015a;b) conducted a numerical analysis on NACA 23012 airfoils with various flap configurations. The results showed an increase in lift but a decrease in the max angle of attack and an increase in the drag coefficient. Arnab *et al.* (2022) compared the aerodynamic performance of NACA 23012 and NACA 4412 airfoils using computational simulations. The flow control was investigated on a NACA 23012 airfoil model using different plasma actuator techniques by Kazanskiy *et al.* (2016). A magnetohydrodynamic plasma actuator was used to study high-speed flow control. The pulsed arc filament generated the Lorentz force along the upper airfoil surface, resulting in changes of up to 5% in average lift and pitching moment at flow velocities of up to 60 $m \cdot s^{-1}$. Alonge *et al.* (2019) investigated flow separation control on the NACA 23012 airfoil using single and double suction. Salam *et al.* (2022) determined the aerodynamic performance of a homebuilt aircraft wing model based on the NACA 23012 airfoil.

Julius *et al.* (2020) enhanced the NACA 23012 airfoil's aerodynamic performance through suction to mitigate flow separation and delay stall. Pouryoussefi *et al.* (2016) investigated the effects of ice accretion on the NACA 23012 airfoil, while König *et al.* (2015) utilized lattice-Boltzmann simulations for complex ice shapes. Badry *et al.* (2013) simulated the effects of glaze ice accretion on the NACA 23012 airfoil.

Moralev *et al.* (2014) aimed to use a surface high-frequency discharge plasma actuator to control lift and drag coefficients at different angles of attack and flow velocities. Reductions of up to 40% in Cx at an angle of attack of 3° and increases of up to 10% in Cy were achieved under specific conditions. The impact on aerodynamic performance occurred at different modulation frequency ranges.

Lasauskas *et al.* (2007) investigated the influence of a trailing-edge tab on moment characteristics, and Zanotti and Gibertini (2013) studied dynamic stall phenomena on an oscillating NACA 23012 airfoil.

Together, these studies highlight the considerable influence of ice buildup on the aerodynamic performance of the NACA 23012 airfoil. The discoveries offer crucial knowledge for comprehending and addressing the effects of ice on aircraft performance, thereby enhancing safety and efficiency during flights in icing conditions. Moreover, these investigations lay a robust foundation for future research in the realms of aerodynamics and airfoil design.

Despite the extensive numerical and flow-control studies available in the literature, reliable low-speed experimental data for a three-dimensional NACA 23012 wing with high-lift devices remain scarce, particularly in the freestream velocity range of 20–50 $m \cdot s^{-1}$ ($Re \approx 0.5 \times 10^6 – 1.3 \times 10^6$). Most existing experimental datasets focus on two-dimensional airfoils, icing effects, or isolated flow-control mechanisms.

The novelty of the present work lies in providing a systematic, uncertainty-quantified experimental database for a half-span NACA 23012 wing, including clean, slat, flap, and combined high-lift configurations. The resulting lift, drag, and pitching moment coefficients are intended to serve as benchmark data for future numerical validation and low-speed aircraft design studies.

# METHODOLOGY

## The wind tunnel

The experiments were carried out in the closed-loop low-speed wind tunnel at the International Islamic University Malaysia. The wind tunnel test section dimensions are 2.30 m (width), 1.50 m (height), and 6.00 m (length). The wind tunnel has a free-stream turbulence intensity of 0.07% in the flow direction, 0.10% in the lateral direction, and 0.11% in the vertical direction. The normal force has a measurement range of ±2000 N, and the axial force measurement range of ±750 N with uncertainties of 0.04% and 0.05%, respectively. The pitching moment has a measurement range of ±250 N·m and 0.04% uncertainty. The measurement uncertainty in lift and drag coefficients is 2%, and the uncertainty in the moment coefficient is 2.5%. The measurements have a confidence level of 95%, and based on this, the uncertainty in velocity is ±0.19 $m \cdot s^{-1}$.

## The model

The half-span wing model used in this work consists of a wing with a tapered NACA 23012 profile, average chord length c = 0.371 m, half-span (b/2) = 0.93 m, and half-wing area S = 0.321 $m^2$. Figure 1 shows the schematic diagram of the half-span wing model. The terms $C_L$, $C_D$, and $C_M$ refer to the lift, drag, and moment coefficients, respectively. The coefficients are obtained from the six-balance forces using the following equations (Anderson 2023):

$$C_L = \frac{L}{q_\infty s} \tag{1}$$

$$C_D = \frac{D}{q_\infty s} \tag{2}$$

$$C_M = \frac{M}{q_\infty cs} \tag{3}$$

where *L* is the lift, *D* is the drag, *M* is the moment, is the dynamic pressure, c is the average chord length, and S is the half-wingspan.

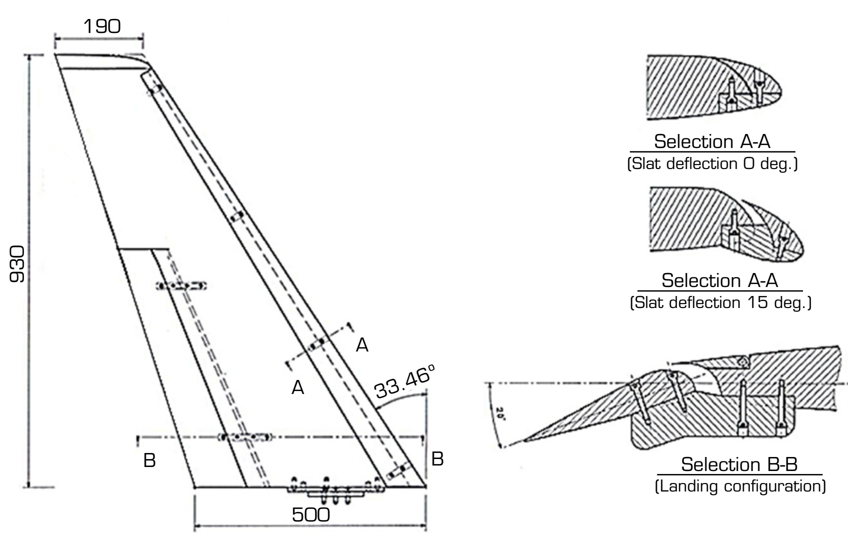


Source: Elaborated by the authors.

**Figure 1.** Schematic diagram of the half-span wing model. Dimensions are in millimeters (mm).

# RESULTS

The aerodynamic performance of the NACA 23012 half-span wing was experimentally evaluated at freestream velocities of 20, 30, 40, and 50 $m \cdot s^{-1}$, corresponding to a low-Reynolds-number regime relevant to light aircraft and high-lift operations. Four configurations were examined: a clean wing, a slat-only configuration, a flap-only configuration, and a combined high-lift configuration incorporating both slat and flap deflections.

Across all configurations, the lift coefficient increased approximately linearly with angle of attack in the pre-stall region, followed by a rapid decline beyond the critical angle of attack, indicating stall onset. Increasing freestream velocity resulted in a systematic increase in maximum lift coefficient and stall angle, consistent with Reynolds-number-dependent boundary-layer behavior. The pitching moment coefficient exhibited a negative slope with respect to angle of attack for all cases, confirming static longitudinal stability of the half-span wing model.

## Clean wing configuration (slat δ = 0°, flap δ = 0°)

For the clean wing configuration, stall occurred between 15° and 18°, depending on freestream velocity. At 20 m·s$^{-1}$, the maximum lift coefficient was $C_{L,max}$ = 1.05 at a critical angle of attack of 15°, increasing progressively to $C_{L,max}$ = 1.24 at 18° for 50 m·s$^{-1}$. This represents an approximate 18% increase in $C_{L,max}$ over the tested velocity range, as shown in Fig. 2.

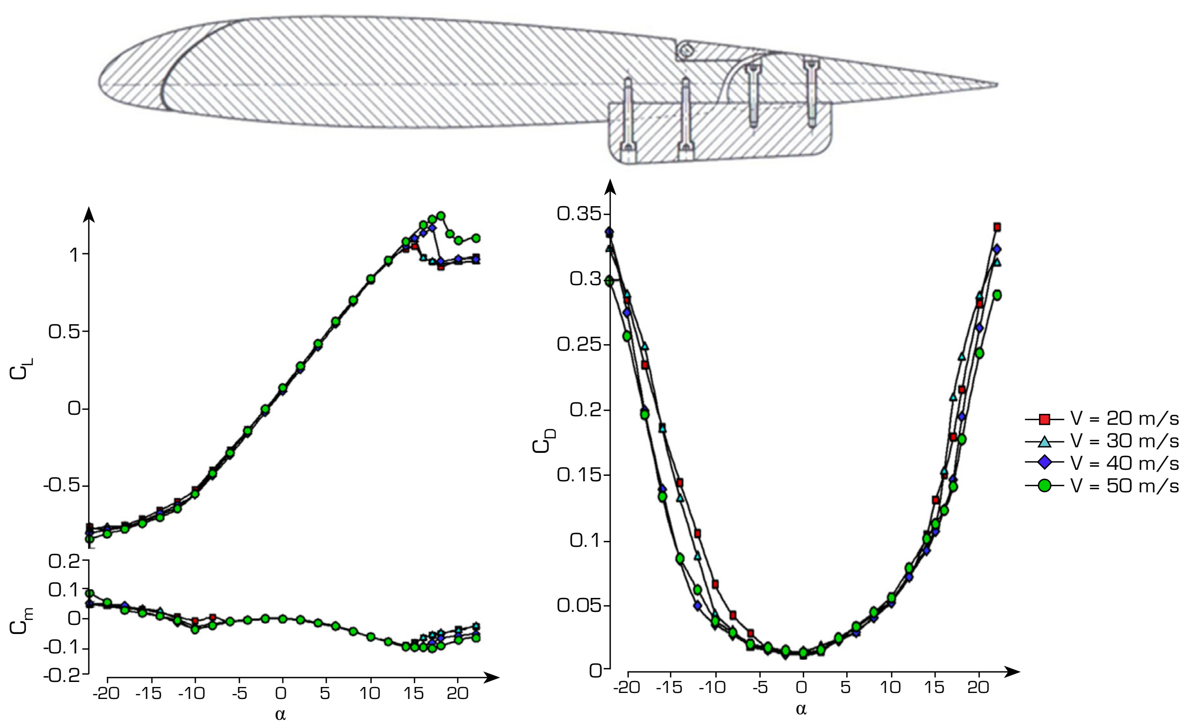


Source: Elaborated by the authors.

**Figure 2.** $C_L$ and $C_D$ vs. α and $C_m$ vs. α for clean wing configuration.

The drag coefficient at stall ranged from $C_D$ = 0.11 to 0.18 as shown in Table 1, increasing with freestream velocity due to higher Reynolds-number effects and increased induced drag at elevated lift levels. The pitching moment coefficient remained negative throughout the tested angle-of-attack range, indicating stable aerodynamic behavior prior to stall. These results are consistent with classical cambered airfoil performance and serve as the baseline for assessing the effectiveness of high-lift devices.

**Table 1.** Aerodynamic performance of NACA 23012 at clean configuration.

| Relative wind speed, V | Critical angle of attack, $\alpha_{critical}$ | Max. CL @ $\alpha_{critical}$ | Max. CD @ $\alpha_{critical}$ |
|---|---|---|---|
| 20 | 15° | 1.05 | 0.13 |
| 30 | 15° | 1.09 | 0.11 |
| 40 | 17° | 1.17 | 0.15 |
| 50 | 18° | 1.24 | 0.18 |

Source: Elaborated by the authors.

## Slat configuration (slat δ = 15°, flap δ = 0°)

The introduction of a leading-edge slat produced a substantial enhancement in aerodynamic performance, particularly in terms of stall delay. The critical angle of attack increased markedly to 23° at 20 $m \cdot s^{-1}$ and up to 28° at higher velocities, representing a stall-angle extension of approximately 10°–13° relative to the clean wing.

The maximum lift coefficient increased to $C_{L,max}$ = 1.39–1.64, corresponding to a 30–35% improvement compared with the clean configuration at similar freestream velocities (Figure 3). This enhancement is attributed to the slat's ability to re-energize the boundary layer over the main wing, thereby delaying flow separation at high angles of attack.

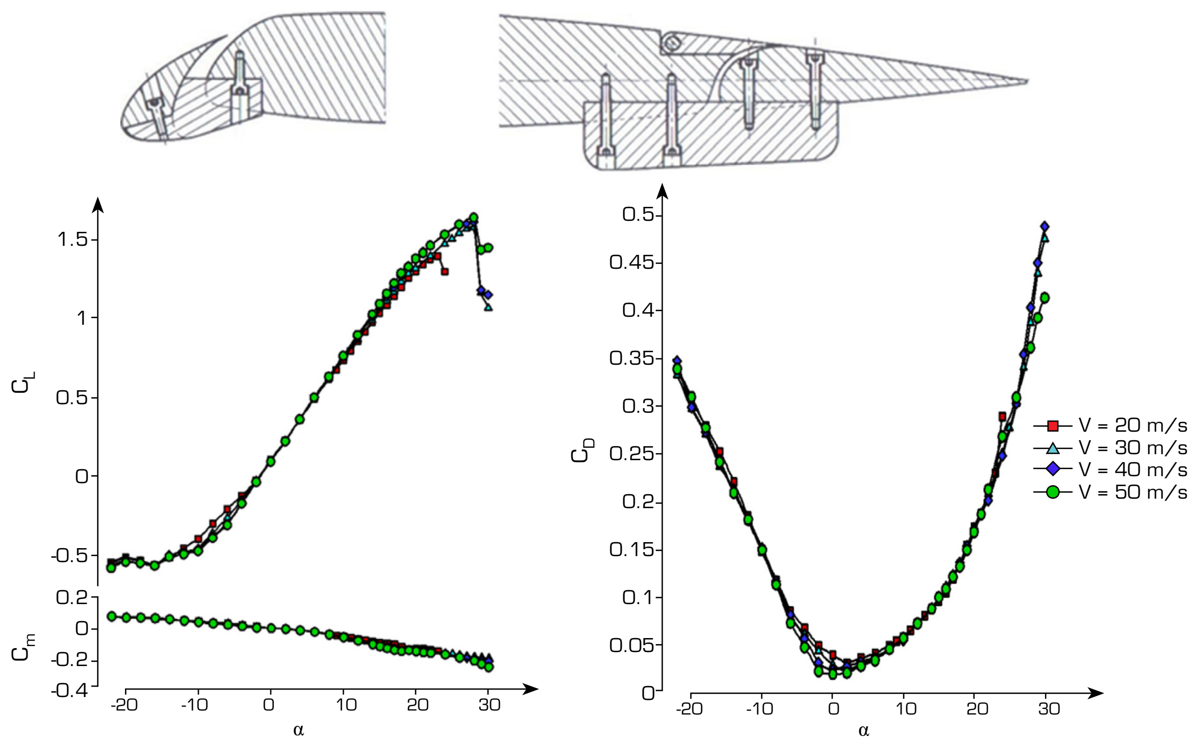


Source: Elaborated by the authors.

**Figure 3.** CL and $C_D$ vs. α and $C_m$ vs. α for slat configuration.

The drag coefficient at stall increased significantly, reaching values between $C_D$ = 0.23 and 0.40, reflecting the aerodynamic penalty associated with slat deployment. Despite this increase, the slat configuration provides a clear advantage for applications requiring high lift and extended operational angles of attack; the critical values of lift and drag coefficients are listed in Table 2.

**Table 2.** Aerodynamic performance of NACA 23012 at slat configuration.

| Relative wind speed, V | Critical angle of attack, $\alpha_{critical}$ | Max. $C_L$ @ $\alpha_{critical}$ | Max. $C_D$ @ $\alpha_{critical}$ |
|---|---|---|---|
| 20 | 23° | 1.39 | 0.23 |
| 30 | 28° | 1.58 | 0.39 |
| 40 | 28° | 1.61 | 0.40 |
| 50 | 28° | 1.64 | 0.36 |

Source: Elaborated by the authors.

## Flap configuration (slat $\delta$ = 0°, flap $\delta$ = 20°)

The trailing-edge flap configuration primarily enhanced lift at lower and moderate angles of attack, without a corresponding delay in stall. For all tested freestream velocities, the critical angle of attack remained approximately 15°, similar to the clean wing configuration.

Based on the results presented in Fig. 4, the maximum lift coefficient increased to $C_{L,max}$ = 1.37–1.52, representing a 25–30% increase over the clean wing. Unlike the slat configuration, the flap primarily increased camber rather than improving boundary-layer attachment, explaining the absence of significant stall-angle extension.

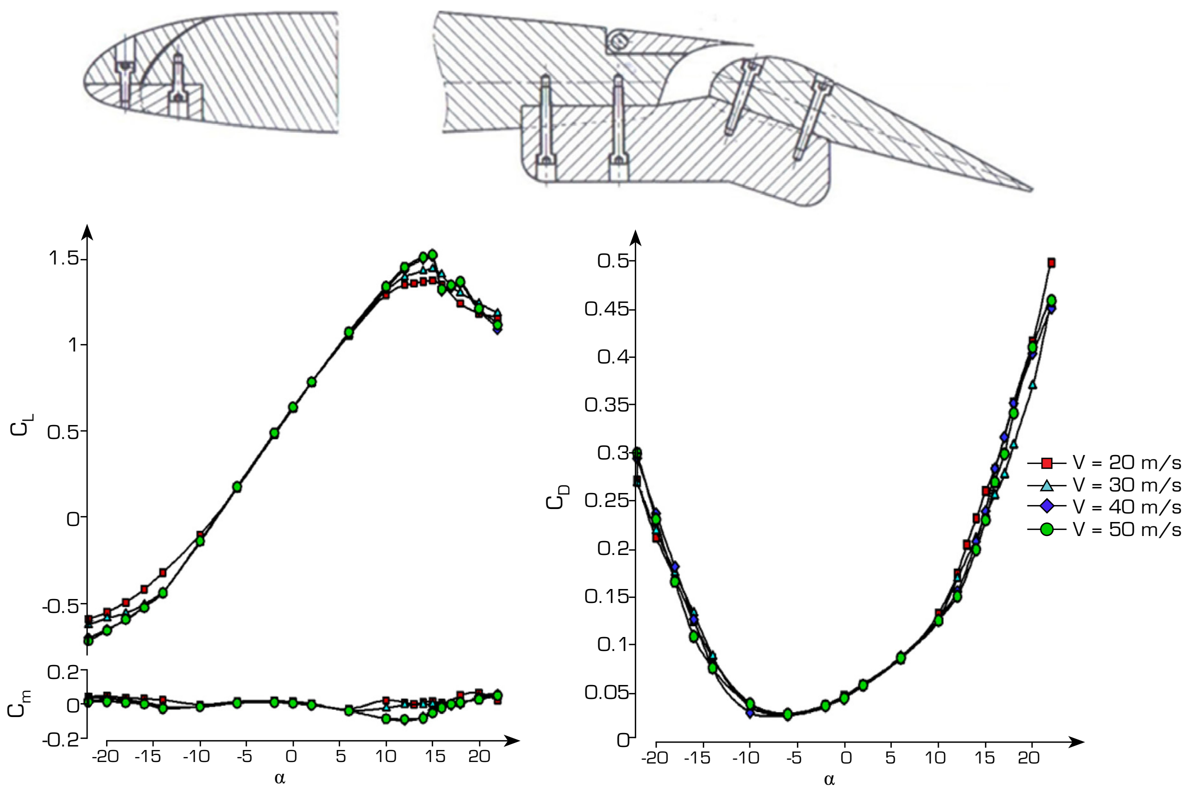


Source: Elaborated by the authors.

**Figure 4.** $C_L$ and $C_D$ vs. α and $C_m$ vs. α for flap configuration.

The drag coefficient at stall ranged from $C_D$ = 0.23 to 0.26 as shown in Table 3, higher than the clean configuration but generally lower than that observed for the slat-only case. These results indicate that flap deployment is effective for increasing lift during takeoff and landing but is less effective for stall mitigation.

**Table 3.** Aerodynamic performance of NACA 23012 at flap configuration.

| Relative wind speed, V | Critical angle of attack, $\alpha_{critical}$ | Max. $C_L$ @ $\alpha_{critical}$ | Max. $C_D$ @ $\alpha_{critical}$ |
|---|---|---|---|
| 20 | 15° | 1.37 | 0.26 |
| 30 | 15° | 1.44 | 0.24 |
| 40 | 15° | 1.51 | 0.24 |
| 50 | 15° | 1.52 | 0.23 |

Source: Elaborated by the authors.

## High-lift configuration (slat δ = 15°, flap δ = 20°)

The combined slat-and-flap configuration delivered the most favorable aerodynamic performance across all tested conditions. Stall occurred between 18° and 21°, representing a 3°–6° increase relative to the clean and flap-only configurations.

The maximum lift coefficient reached values of $C_{L,max}$ = 1.68–1.86, corresponding to a 60–70% increase compared with the clean wing. This substantial improvement results from the combined effects of boundary-layer re-energization by the slat and increased camber due to the flap.

The drag coefficient at stall ranged from $C_D$ = 0.26 to 0.31 as shown in Table 4, reflecting the cumulative drag contribution of both high-lift devices, as shown in Fig. 5. Nevertheless, the lift gains achieved outweigh the drag penalties in low-speed, high-lift operational regimes, making this configuration particularly suitable for short takeoff and landing applications.

**Table 4.** Aerodynamic performance of NACA 23012 at high lift configuration.

| Relative wind speed, V | Critical angle of attack, $\alpha_{critical}$ | Max. $C_L$ @ $\alpha_{critical}$ | Max. $C_D$ @ $\alpha_{critical}$ |
|---|---|---|---|
| 20 | 18° | 1.68 | 0.26 |
| 30 | 19° | 1.75 | 0.27 |
| 40 | 20° | 1.84 | 0.29 |
| 50 | 21° | 1.86 | 0.31 |

Source: Elaborated by the authors.

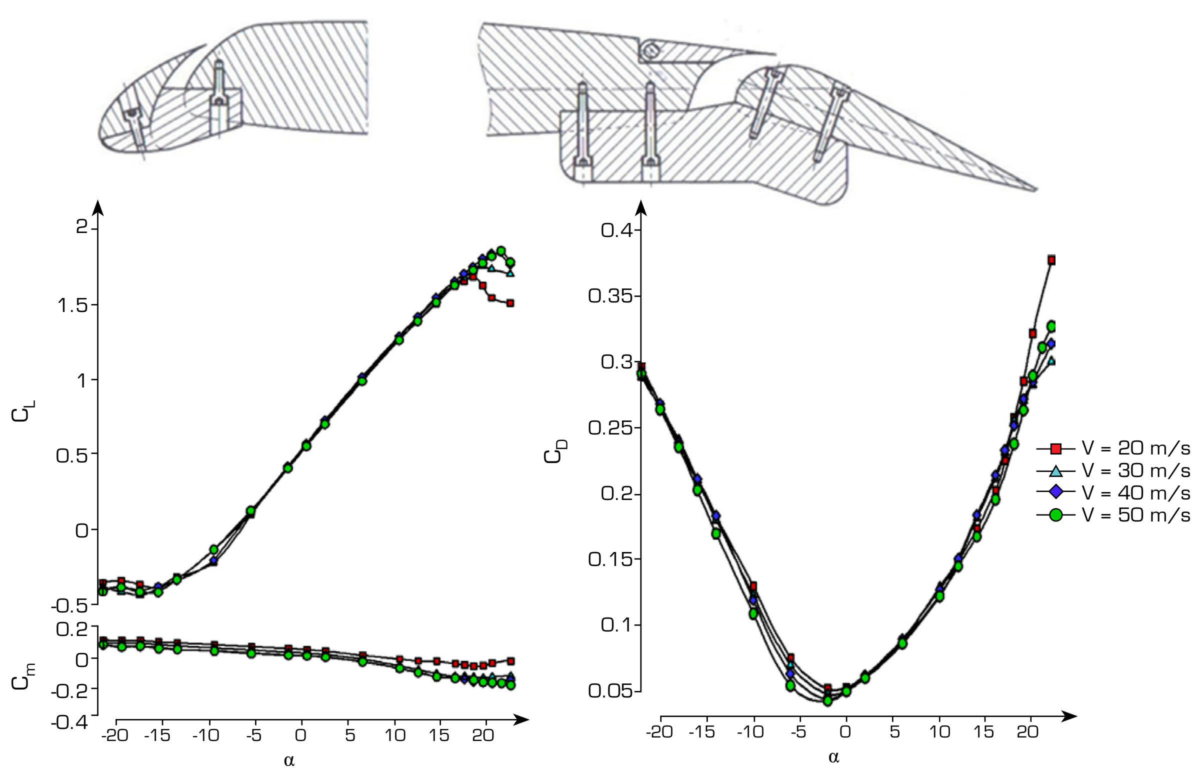


Source: Elaborated by the authors.

**Figure 5.** $C_L$ and $C_D$ vs. α and $C_m$ vs. α for high lift configuration.

The experimentally measured stall angles for the clean wing configuration ranged from 15° to 18°. When compared with the representative stall angle of approximately 17° reported by Anderson (2023) for cambered airfoils at similar Reynolds numbers, the mean experimental stall angle (16.5°) differs by approximately 3%, demonstrating good agreement and supporting the accuracy of the present experimental methodology.

## CONCLUSION

This experimental study demonstrates the significant aerodynamic benefits of high-lift devices on a NACA 23012 half-span wing at low freestream velocities (20–50 $m \cdot s^{-1}$). Relative to the clean configuration, the slat increased $C_{L,max}$ by up to 35% and delayed stall by approximately 10°–13°, while the flap increased lift by up to 30% without extending the stall angle.

The combined high-lift configuration yielded the most favorable performance, with $C_{L,max}$ increases of up to 70% and stall-angle extensions of 3°–6° compared with the clean wing. Although drag increased for all high-lift configurations, the resulting lift-to-drag characteristics remain advantageous for low-speed flight and takeoff/landing conditions.

The presented dataset, validated against classical aerodynamic theory, provides a benchmark experimental reference for future numerical simulations and low-speed aircraft design involving the NACA 23012 airfoil.

## CONFLICTS OF INTEREST

Nothing to declare

## AUTHOR CONTRIBUTIONS

**Conceptualization:** Altaf A; **Methodology:** Altaf A; **Software:** Altaf A; **Validation:** Altaf A, Aldheeb MAM, Omar AA, and Asrar W; **Formal Analysis:** Altaf A, Aldheeb MAM, Omar AA, and Asrar W; **Investigation:** Altaf A; **Data Curation:** Altaf A; **Writing – Original Draft:** Altaf A; **Writing – Review & Editing:** Aldheeb MAM, Omar AA, and Asrar W; **Supervision:** Omar AA and Asrar W; **Project Administration:** Altaf A, Aldheeb MAM, Omar AA, and Asrar W; **Final approval:** Aldheeb MAM.

## DATA AVAILABILITY STATEMENT

The data will be available upon request.

## FUNDING

Not applicable

## DECLARATION OF USE OF ARTIFICIAL INTELLIGENCE TOOLS

During the preparation of this manuscript, the authors have used the assistance of the artificial intelligence tool Qwen3.6-Plus in enhancing language, correcting grammar errors, and improving overall readability. The authors carefully reviewed, revised, and validated all generated suggestions. The authors take full responsibility for the final content of the publication.

## ACKNOWLEDGEMENTS

Not applicable

# REFERENCES


Addy HE Jr, Broeren AP, Potapczuk MG, Lee S, Guffond D, Montreuil E, Moens F (2016) Ice accretions and full-scale iced aerodynamic performance data for a two-dimensional NACA 23012 airfoil. NASA/TP-2016-218348.

Alonge OI, Akinneye AO, Julius MO (2019) Stall control on the NACA 23012 airfoil via single and double suction. Paper presented 2019 1st International Conference on Engineering and Environmental Sciences. Osun State University; Osogbo, Nigeria. https://shorturl.at/XiWuv

Anderson JD (2023) Fundamentals of aerodynamics. 6th ed. New York: McGraw-Hill.

Arnab MB, Inam MI (2022) Comparison of aerodynamic performance of NACA 23012 and NACA 4412 airfoil: a numerical approach. Paper presented 2022 International Conference on Mechanical, Industrial, and Energy Engineering. ICMIEE; Khulna, Banglades. https://doi/org10.5281/zenodo.7710580

Badry AH, El-Banna HM, El-Sayed AF, Salem GB (2013) Computational investigation (simulation) of flow field and aerodynamic analysis over NACA 23012 airfoil with leading edge glaze ice shape. Paper presented 2013 Eleventh International Conference of Fluid Dynamics. Military Technical College; Cairo, Egypt. https://shorturl.at/rDNsG

Cavanaugh M, Robertson P, Mason WH (2007) Wind tunnel test of Gurney flaps and T-strips on an NACA 23012 wing. Paper presented 2007 25th AIAA Applied Aerodynamics Conference. AIAA; Miami, USA. https://doi.org/10.2514/6.2007-4175

Gabbasa A, Jawad B, Liu L, Arslan S (2013) Numerical study of the aerodynamic characteristics of a multi-element airfoil NACA 23012. SAE Int J Aerosp 6:8-16. https://doi.org/10.4271/2013-01-1410

Julius MO, Adio SA, Muritala AO, Alonge OI (2020) The suction control characteristics of flow separation on NACA 23012. East Afr J Eng 2(1):1-13. https://doi.org/10.37284/eaje.2.1.121

Jun G, Oliden D, Potapczuk MG, Tsao JC (2014) Computational aerodynamic analysis of three-dimensional ice shapes on a NACA 23012 airfoil. Paper presented 2014 6th AIAA Atmospheric and Space Environments Conference. AIAA; Atlanta, USA. https://doi.org/10.2514/6.2014-2202

Kazanskiy PN, Moralev IA, Bityurin VA, Efimov AV (2016) Active flow control on a NACA 23012 airfoil model by means of magnetohydrodynamic plasma actuator. J Phys Conf Ser 774(1):012153. https://doi.org/10.1088/1742-6596/774/1/012153

König B, Fares E, Broeren AP (2015) Lattice-Boltzmann analysis of three-dimensional ice shapes on a NACA 23012 airfoil. SAE Tech Pap 2015-01-2084. https://doi.org/10.4271/2015-01-2084

Lasauskas E, Lutz T, Dietz M (2007) Influence of trailing edge tab on moment characteristics of NACA 23012 airfoil. Aviation 11(4):3-8. https://doi.org/10.3846/16487788.2007.9635970

Moralev I, Klimov A, Bityurin V, Kazansky P (2014) Lift and drag control of NACA 23012 airfoil model by surface HF plasma actuator. Paper presented 2014 52nd AIAA Aerospace Sciences Meeting. AIAA; National Harbor, USA. https://doi.org/10.2514/6.2014-1263

Pouryoussefi SG, Mirzaei M, Nazemi MM, Fouladi M, Doostmahmoudi A (2016) Experimental study of ice accretion effects on aerodynamic performance of an NACA 23012 airfoil. Chin J Aeronaut 29(3):585-595. https://doi.org/10.1016/j.cja.2016.03.002

Salam N, Tarakka R, Jalaluddin, Iriansyah D, Ihsan M (2022) The effects of flap angles on the aerodynamic performances of a homebuilt aircraft wing model. Int J Mech Eng Robot Res 11(12):908-914. https://doi.org/10.18178/ijmerr.11.12.908-914

Todorov M (2015a) Aerodynamic characteristics of airfoil with single plain flap for light airplane wing. Paper presented 2015 International Conference on Military Technologies. IEEE; Brno, Czech Republic. https://doi.org/10.1109/MILTECHS.2015.7153648

Todorov M (2015b) Aerodynamic characteristics of airfoil with single slotted flap for light airplane wing. Paper presented 2015 Air Force Academy Scientific Session. AFASES; Brașov, Romania. https://doi.org/10.1109/MILTECHS.2015.7153648

Yoo NS (2000) Effect of the Gurney flap on a NACA 23012 airfoil. KSME Int J 14:1013-1019. https://doi.org/10.1007/BF03185804

Zanotti A, Gibertini G, Grassi D, Spreafico D (2013). Wake measurements behind an oscillating airfoil in dynamic stall conditions. International Scholarly Research Notices 2013(1), 265429. https://doi.org/10.1155/2013/265429